Available online at www.sciencedirect.com
SCIENCE DIRECT
Polymer 46 (2005) 12440–12451
polymer
www.elsevier.com/locate/polymer

Controlling the miscibility of polyethylene/layered silicate nanocomposites by altering the polymer/surface interactions

K. Chrissopoulou [a,b,*], I. Altintzi [a,c], S.H. Anastasiadis [a,c], E.P. Giannelis [d], M. Pitsikalis [e], N. Hadjichristidis [e], N. Theophilou [f]

[a] *Institute of Electronic Structure and Laser, Foundation for Research and Technology-Hellas, P.O. Box 1527, 71110 Heraklion Crete, Greece*
[b] *Department of Materials Science and Technology, University of Crete, 710 03 Heraklion Crete, Greece*
[c] *Department of Physics, University of Crete, 710 03 Heraklion Crete, Greece*
[d] *Department of Materials Science and Engineering, Cornell University, Ithaca, NY 14853, USA*
[e] *Department of Chemistry, University of Athens, 157 01 Zografou, Athens, Greece*
[f] *R&D Center, S&B Industrial Minerals S.A., 145 64 Kifisia, Athens, Greece*

Received 16 August 2005; received in revised form 17 October 2005; accepted 24 October 2005
Available online 14 November 2005

Abstract

Polyethylene/layered silicate nanocomposites are synthesized utilizing three types of polymeric surfactants/compatibilizers in order to influence the miscibility of polyethylene with the nanoparticle surface. The additives are designed so that they can play the role of a polymeric surfactant modifying the hydrophilic clay or of a compatibilizer with the organoclay. Model additives, especially synthesized for this study, included: polyethylene chains, which possess either a single functional end-group or multiple functional groups along the chain, as well as functional diblock copolymers. Maleic anhydrite grafted polyethylene with a low degree of functionalization was used as well. The structure of the resulting micro- or nanocomposites was investigated by X-ray diffraction and transmission electron microscopy. Immiscible hybrids as well as intercalated and/or exfoliated nanocomposites are obtained in a controlled way, depending on the kind of additive and its concentration in the mixture. The most important factor controlling the structure and the properties is the ratio of additive to nanoparticles. The rheological properties of the hybrids correlate well with the final micro- or nanostructure.

Keywords: Polyethylene nanocomposites; Polymeric surfactants/compatibilizers; Surface interactions

1. Introduction

Addition of inorganic materials in a polymeric matrix is a very common approach to optimize properties [1]. It is expected that certain problems frequently encountered due to the large size (~a few microns) of the inorganic additives (like reduction of transparency or reduced toughness) would be overcome if the inorganic exists as a fine dispersion within the polymeric matrix, i.e., when its dimensions are of the order of a few nanometers, producing a nanocomposite. In these cases the final properties of the hybrid are determined mainly by the existence of many interfaces [2]. A special case of nanocomposites is obtained [3–6] by mixing polymers with layered silicates (nanoclays) where three different types of structure can be identified depending on the interactions between the polymer and the inorganic nanoparticles: phase separated, where the polymer and the inorganic are mutually immiscible, intercalated, where the polymer chains intercalate between the layers of the inorganic material, and exfoliated, where the periodicity of the inorganic material is destroyed and the inorganic platelets are dispersed within the polymeric matrix. Achieving the desired structure is a scientific problem with numerous technological implications because it is the structure that controls the final properties of the micro- or nanocomposites [7,8]. Such nanocomposites exhibit remarkable improvement in a variety of properties like strength and heat resistance [9], gas permeability [10–13], flammability [14,15] and biodegradability [16]. The superior properties of the nanocomposites are attributed to the high aspect ratio of the inorganic layers giving rise to a high degree of polymer–clay surface interactions [3,10,17].

* Corresponding author. Address: Institute of Electronic Structure and Laser, Foundation for Research and Technology-Hellas, P.O. Box 1527, 71110 Heraklion Crete, Greece. Tel.: +30 2810 391255; fax: +30 2810 391305.
E-mail address: kiki@iesl.forth.gr (K. Chrissopoulou).

0032-3861/$ - see front matter © 2005 Elsevier Ltd. All rights reserved.
doi:10.1016/j.polymer.2005.10.106

The layered silicate nanoparticles are usually hydrophilic and their interactions with non-polar polymers are not favorable. Thus, whereas, hydrophilic polymers are likely to intercalate within Na-activated montmorillonite clays [18], hydrophobic polymers can lead to intercalated [17,19] or exfoliated [20] structures only with organophilized clays, i.e., with materials where the hydrated Na^+ within the galleries has been replaced by proper cationic surfactants (e.g. alkylammonium) by a cation exchange reaction.

The thermodynamics of intercalation or exfoliation have been discussed [21–24] in terms of both enthalpic and entropic contributions to the free energy. It has been recognized that the entropy loss due to the polymer confinement is compensated by the entropy gain associated with the increased conformational freedom of the surfactant tails as the interlayer distance increases with polymer intercalation [21,25], whereas, the favorable enthalpic interactions are extremely critical in determining the nanocomposite structure [26].

Polyolefins constitute an important class of polymers with applications ranging from packaging to automotive. Attempts to develop either intercalated or exfoliated nanocomposite structures with polypropylene [15,27–34] or polyethylene [35–40] have not been particularly successful due to the strong hydrophobic character of the polymers and the lack of favorable interactions with the silicate surfaces. Synthetic efforts have focused on the introduction of functional groups to the polyolefin chains, on altering the organophilization of the inorganic or on the use of suitable compatibilizers, like a maleic anhydrite functionalized polyolefin. Alternatively, polyolefin nanocomposites can be prepared by an in situ polymerization of the proper monomers around dispersed inorganic layers [41–43].

There is a rich literature on polyethylene nanocomposites; however, in most cases the reported results are not consistent. Most of the studies report exfoliation of the silicate structure, when maleic anhydrite functionalized polyethylene is used either as a compatibilizer or as the polymer [35,36,38], especially for high ratios of compatibilizer to organoclay. Exfoliation or intercalation is reported depending on the degree of functionalization of the maleic anhydrite and the chain length of the organic modifier [39]. Four different morphologies, intercalated, mixed intercalated and exfoliated, ordered exfoliated and disordered exfoliated, have been observed, in this sequence as the concentration of silicate decreases [40]. Even for unmodified polyethylene, there are conflicting reports on intercalation [39] besides those reporting immiscible systems [35].

In this paper, we aim at controlling the miscibility of polyethylene with inorganic layered silicate nanoparticles by altering the polymer–surface interactions. To that end, a series of additives have been utilized, either specifically synthesized for this project or commercially available. These additives are designed so that they can play the role of a polymeric surfactant, when mixed with hydrophilic clay or they may act as a compatibilizer when mixed with an organophilized one. Three types of additives have been designed for this purpose. Polyethylene chains functionalized by dimethyl ammonium chloride either as a single end-group or as multiple functional groups along the chain are one type of additives synthesized by anionic polymerization of butadiene and subsequent hydrogenation to produce polyethylene. The second type of additive is a diblock copolymer of polyethylene-*block*-poly(methacrylic acid) also synthesized anionically followed by hydrogenation and deprotection of the methacrylic acid. The third type is based on the widely used maleic anhydride grafted polyethylene with a low degree of functionalization. Immiscible, intercalated and exfoliated structures can be obtained in a controlled way, which depends on the kind of additive and its concentration in the mixture. It is shown that the most important factor controlling the structure is the ratio of additive to inorganic. The structure of the resulting micro- or nanocomposites was investigated by X-ray diffraction and transmission electron microscopy. In addition, the rheological behavior of the different systems has been studied and the resulting properties were found to correlate well with the micro- or nanostructure of the materials.

2. Experimental section

2.1. Materials

The synthesis of the polyethylene-based model macromolecular surfactants and compatibilizers was performed utilizing anionic polymerization under high vacuum [44] followed by the appropriate post-polymerization reactions in order to introduce or reveal the desired functional moieties.

All monomers (butadiene, Bd, *t*-butyl methacrylate, *t*BuMA, 1,1-diphenyl ethylene, DPE), solvents (benzene, hexane and tetrahydrofuran, THF), tetramethylene ethylene diamine, (TMEDA) and the termination agent MeOH were purified to the standards required for high-vacuum anionic polymerization techniques. *sec*-Butyllithium (*s*-BuLi) was prepared from *sec*-butyl chloride and lithium dispersion. Dimethylaminopropyl lithium (DMAPLi) was prepared [45] under vacuum from the corresponding chloride and lithium dispersion, whereas, trioctylaluminum (TOA), Pd on $CaCO_3$, and calcium hydride (CaH_2), were used as received.

Polyethylenes with quaternized amine end-groups were synthesized as follows: butadiene was polymerized anionically under high vacuum using DMAPLi as initiator and benzene solvent in order to obtain polybutadiene with high 1,4 microstructure. The living polymer was terminated with MeOH, precipitated in MeOH and dried thoroughly under vacuum, to give the sample NPB. The polymer was then dissolved in cyclohexane to give a 10% solution and was placed in a Parr autoclave. The sample was hydrogenated using Pd on $CaCO_3$, as the heterogeneous catalyst at 100 °C and at hydrogen pressure 400 psi. High purity hydrogen (99.999%) was employed, and the reaction was allowed to take place overnight. The solution was then filtered twice, while still hot, using 90 mm millipore filters. A final filtration with 0.45 mm filters provided the pure and colorless NPE sample. The hydrogenation reaction was quantitative as evidenced by ^1H NMR spectroscopy (absence of the double bond signals).

The dimethylamine end-groups were quaternized using excess of concentrated HCl.

Polyethylene with multiple quaternized amine groups along the polymer chain was obtained as follows. Linear PBd prepared by anionic polymerization, with $M_w = 110{,}600$ was introduced into a specially designed glass apparatus, which was then attached to the high vacuum line. The polymer was allowed to stand under vacuum overnight in order to remove volatile impurities. Benzene was then distilled through the vacuum line to give a 10% polymer solution. The apparatus was sealed-off from the vacuum line, and the polymer was allowed to dissolve at room temperature. An equimolar amount of TMEDA and *s*-BuLi was then added. The lithiation reaction was allowed to proceed for 4 h at room temperature, under continuous stirring. The multifunctional initiator was then employed to initiate the polymerization of a new small quantity of butadiene, dissolved in benzene. The polymerization was terminated after 24 h using dimethylaminopropyl chloride. (DMAPCl), resulting in the formation of a comb polybutadiene, PBd-*g*-NPBd, which has branches end-functionalized with dimethylamine groups. The pure product was obtained by fractionation using toluene/methanol as the solvent/non-solvent system. The PBd-*g*-NPBd comb was hydrogenated by heterogeneous catalysis, as before. The functionalized PE-*g*-NPE comb, thus produced, was dissolved in trichlorobenzene at 130 °C and was quaternized using an excess of HCl. The procedure is shown in Scheme 1. The restrictions of the synthetic method do not allow for the exact determination of the number of branches of the comb polymer. However, the ^{1}H NMR spectrum shows a peak at 2.2 ppm, attributed to the $-CH_3$ groups that belong to the dimethylamine functions. Comparison of this signal with the signal of the main chain protons leads to the estimation that 15 dimethylamine groups have been incorporated to the comb structure. Judging from this result and the small increase of the molecular weight of the PBd backbone after the grafting reaction, it can be concluded that each of the branches is actually an oligomer. Therefore, the final structure can be considered as a linear polymer having multiple dimethylamine groups along the macromolecular chain.

Finally, polyethylene-*b*-poly(methacrylic acid), PE-*b*-PMAA diblock copolymer was synthesized by sequential addition of monomers. Butadiene was polymerized anionically in benzene using *sec*-BuLi as initiator. The living polymer solution was concentrated to 25–30% w/v by distilling part of the solvent through the vacuum line. The remaining solution was collected in a flask with break-seal and was attached to the reactor for the polymerization of *t*BuMA. THF was distilled into the polymerization flask in order to give a benzene/THF = l:3 (v/v) solution. DPE was added and allowed to react with the PBdLi solution for 15 min followed by the addition of a five-fold excess of LiCl, dissolved in THF, over the living ends. *t*BuMA was then distilled and the polymerization was performed at −78 °C in order to obtain the living PBd-*b*-PtBuMA copolymer. The living polymer was finally terminated with MeOH. Selective hydrogenation of the PBd block of the copolymer was achieved by homogeneous catalytic hydrogenation in toluene solutions using the Wilkinson catalyst, $(PPh_3)_3RhCl$ (100 ppm), and a Parr autoclave. The reaction took place at 100 °C and at hydrogen pressure 400 psi.

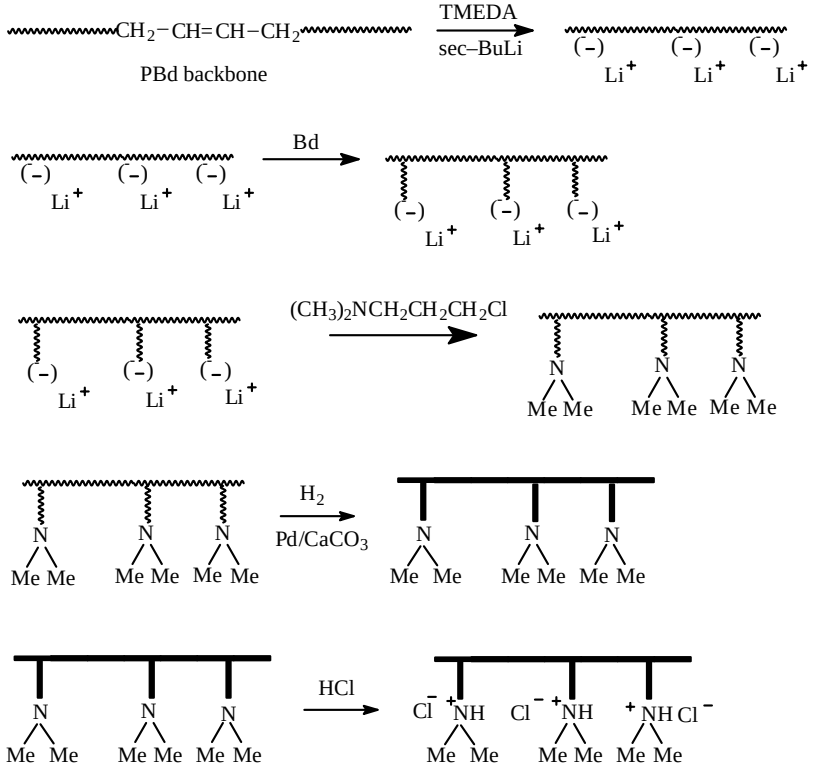

Scheme 1. Synthesis of PE combs with quaternized amine end-groups in each branch.

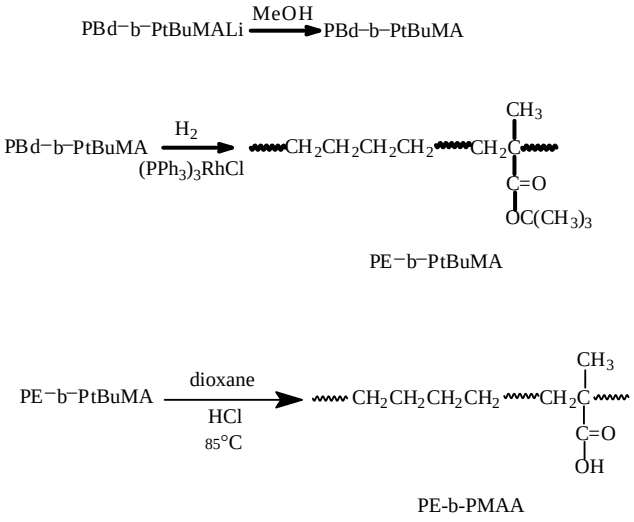

Scheme 2. Synthesis of the PE-*b*-PMAA block copolymer.

The PE-*b*-PtBuMA copolymer thus prepared, was dispersed in dioxane and was heated at 85 °C in the presence of concentrated HCl for several hours to give the PE-*b*-PMAA copolymer. The procedure is shown in Scheme 2.

The synthesized polymers were characterized by size exclusion chromatography and static light scattering in THF and by ^{1}H NMR in *d*-chloroform (at 30 °C). Their macromolecular characteristics are shown in Table 1. It is evident that narrow molecular weight distribution polymers were obtained in all cases. Note that in all cases the sample characteristics were measured before the post polymerization reactions (hydrogenation and hydrolysis) which have been tested to be quantitative [46].

A maleic anhydride grafted polyethylene with 0.85% functional maleic anhydride groups and a melt-flow index (MFI) of 1.5 was purchased from Aldrich and was used as received.

An injection grade linear low density polyethylene (SABIC) with a melt-flow index (MFI) of 37 was used. A variety of silicates including two hydrophilic montmorillonites, Na^+MMT (Laviosa Chimica Mineraria) and Cloisite Na^+ (Southern clay) as well as two organoclays, Dellite 72 T (Laviosa Chimica Mineraria) and Cloisite 20 A (Southern clay) were used. The organosilicates are based on especially purified montmorillonite, organophilized via a cation exchange reaction using dimethyl dihydrogenated tallow quaternary ammonium chloride as the organic modifier. Hydrogenated tallow is a product consisting of a distribution of hydrocarbon chains with approximate composition 65% C18; 30% C16; 5% C14. Thermogravitometric analysis (TGA) measurements performed, showed that for Dellite 72 T there is a 37.1 wt% loss of weight between 220 and 440 °C, whereas, for Cloisite 20 A there is 32.3 wt% loss of weight between 200 and 435 °C which is attributed to the decomposition of the surfactants.

Specifics of the polymeric compatibilizers and the silicate nanoparticle are shown in Tables 1 and 2, respectively.

Table 1
Characteristics of the polymeric surfactants/compatibilizers

Type of additive	Code	M_w[a]	$I=M_w/M_n$[b]
N-PBd	NPBd-1	9,700	1.04
	NPBd-2	22,900	1.04
PBd-*b*-PtBuMA	PBd-*block*	4,800	1.05
	PBd-*b*-PtBu-MA[c]	13,800	1.06
PBd-*g*-NPBd	PBd backbone	110,600	1.03
	NPBd branch	500[d]	
	PBd-*g*-NPBd	118,100	1.03

[a] By low angle laser light scattering in THF at 25 °C.
[b] By size exclusion chromatography in THF at 40 °C.
[c] 34.8 wt% in PBd by ^{1}H NMR.
[d] Calculated from the molecular weight of the backbone, the total molecular weight and the number of branches as was estimated by ^{1}H NMR.

2.2. Experimental techniques

2.2.1. Micro-extruder

A DSM 5 cm^3 twin screw micro-mixer and micro-extruder was utilized in order to facilitate the melt mixing of the polymers with the inorganic nanoparticles as well as with the additives. The polymer was initially placed into the mixer and was left to melt and homogenize at 150 °C and 100 rpm for ~5 min. The inorganic material was subsequently introduced in the appropriate amount so that its concentration in the mixture would be 5–15 wt%. Following homogenization of the mixture for ~20 min, the specimens were obtained in the form of cylindrical extrudates of 1–3 mm in diameter. TGA

Table 2
Inorganic layered silicates characteristics

Code	Sample	d_{001} (Å)	Source
Na^+MMT	Hydrophilic montmorillonite	9.9	Laviosa
Cloisite Na^+	Hydrophilic montmorillonite	9.9	Southern clay
Dellite 72 T	Organophilic montmorillonite	30.4	Laviosa
Cloisite 20 A	Organophilic montmorillonite	25.9	Southern clay

experiments verify that at the temperature of sample preparation, no degradation of either the polymer or the surfactants occur.

2.2.2. X-ray diffraction

Structural characterization of the nanocomposites was performed with X-ray diffraction, using a RINT-2000 Rigaku diffractometer. The X-rays are produced by a 12 kW rotating anode generator with a Cu anode equipped with a secondary pyrolytic graphite monochromator. The Cu Kα radiation was used with wavelength $\lambda = \lambda_{\text{Cu K}\alpha} = 1.54$ Å. Measurements were performed for 2θ from 1.5 to 30° with step of 0.02°. The organoclays were measured in a powder form whereas the pure polymer and the nanocomposites in sample holders suitable for the cylindrical extrudates. Materials with periodic structure like the layered silicate clays show characteristic (001) diffraction peaks which are related to the spacing of the layers according to Bragg's law, $n\lambda = 2d_{001}\sin\theta$, where λ is the wavelength of the radiation, d_{001} is the interlayer distance and 2θ is the diffraction angle. It is expected, that, when the polymer is intercalated within the layers of the inorganic material, there will be an increase in the interlayer distance, resulting in a shift of the diffraction angles towards lower values. In the case of exfoliated nanocomposites, the layered structure will be destroyed and the diffraction peaks will disappear.

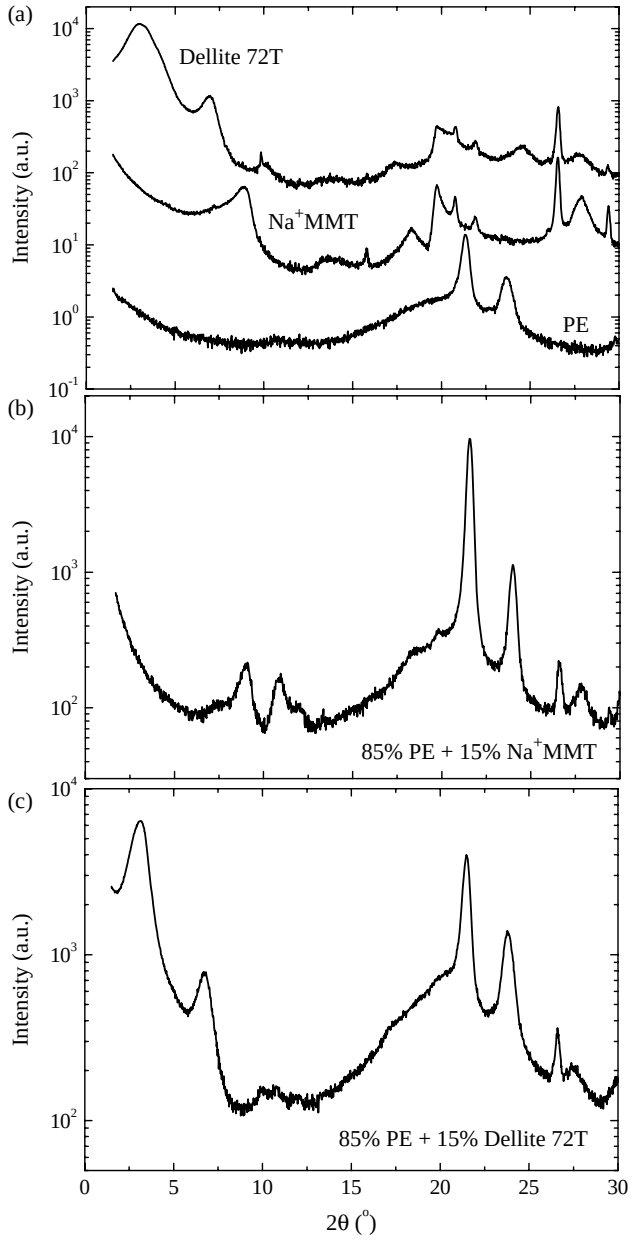

Fig. 1. (a) X-ray diffractograms of polyethylene (PE), hydrophilic clay (Na^+MMT) and organophilic clay (Dellite 72 T). The curves are shifted for clarity. (b) X-ray diffractogram of a micro-composite with 85 wt% PE + 15% Na^+ MMT. (c) X-ray diffractogram of a micro-composite with 85 wt% PE + 15 wt% Dellite 72 T.

2.2.3. Transmission electron microscopy

Bright field TEM images of PE/layered silicate nanocomposites were obtained at 120 kV under low-dose conditions, with a Philips 400 T microscope. The nanocomposite samples were cryomicrotomed with a diamond knife at −110 °C to give sections with a nominal thickness of 70 nm. The contrast between the silicon-containing phase (shown as dark lines) and the polymer (bright region) was sufficient for imaging, and no further staining was required.

2.2.4. Rheology

The rheological properties of the micro- and nanohybrids were investigated utilizing a Rheometrics Scientific ARES strain controlled rheometer. All measurements were performed in parallel plate geometry with plates of 8 or 25 mm in diameter. The sample thicknesses varied between 1 and 2 mm. In all the cases, an isothermal time sweep was initially performed to ensure the dynamic equilibrium of the samples followed by dynamic strain sweeps for strains between 1 and 100% at specific frequencies in order to define the limits of the linear viscoelastic regime. Finally, dynamic frequency sweeps were performed and the storage G' and loss G'' moduli were measured as a function of frequency for constant strain.

3. Results and discussion

Fig. 1 shows X-ray diffractograms of the pure materials and their composites. Two main diffraction peaks are evident in the polyethylene homopolymer at $2\theta_1 = 21.3°$ and at $2\theta_2 = 23.7°$ corresponding to the d_{110} and the d_{200} peaks of the orthorhombic crystal structure of polyethylene with the d_{110} possessing higher intensity [47]. The data for the purified montomorillonite (Na^+ MMT, Laviosa) show a main peak at $2\theta = 8.9°$, which corresponds to an interlayer distance of $d_{001} = 9.9$ Å. Similar results are obtained with Cloisite Na^+ montmorillonite (Southern clay). Note that this sample was kept in a vacuum oven overnight at 150 °C in order to remove the water that was absorbed due to the sample's hydrophilic character [48]. The data for the organoclay, Dellite 72 T, is shown in the same figure. The organoclay shows its main peak at $2\theta = 2.9°$ which corresponds to $d_{001} = 30.4$ Å. The fact that the first and second maxima are not exactly equidistant in the

2θ scale may be attributed to a possible random interstratification of the organoclay platelets [49]. It is noted that the d_{001} spacing of the frequently used Cloisite 20 A organoclay, which is organophilized with the same surfactants, is only $d_{001}=$ 25.9 Å. This indicates the existence of excess surfactant chains inside the galleries of Dellite 72 T since such a large difference cannot be due to random interstratification. Indeed, when Dellite 72 T was washed three times with ethanol, centrifuged, filtered and then dried, its d_{001} spacing became $d_{001}=25.2$ Å, which is similar to that of Cloisite 20 A. The peaks observed in the spectra of both clay and organoclay at angles higher than $2\theta\sim25°$ are due to remaining minute impurities even after the purification process; for example, the peak at $2\theta\sim26.5°$ indicates the presence of quartz. Comparison between the diffractograms of the hydrophilic and the organophilic clays shows that the incorporation of the surfactants leads to an increase of the interlayer spacing by more than 10 Å. In addition, the peaks corresponding to the nanoparticles appear in a different angle range than those corresponding to the polymer, which makes the identification of any intercalation obvious.

Fig. 1(b) and (c) shows X-ray diffractograms for microcomposites prepared by melt mixing PE with a hydrophilic (Na^+ MMT) and a hydrophobic (Dellite 72 T) clay, respectively. The mixing was performed with the microextruder at 150 °C. It is evident that there is not any indication for either intercalation of the polymer chains or exfoliation of the clay layers with neither the clay nor the organoclay. The main diffraction peaks appear at the same angles with those of the pure inorganic materials. Varying the concentration of the silicate from 15 to 5 wt% does not alter the results. The immiscibility of the PE/hydrophilic clay is of course anticipated but it is shown here as a reference for the later experiments with the synthesized additives. Moreover, it is noted that polystyrene intercalates readily with the organoclay Dellite 72 T because of its favorable interactions with the silicate surface. However, this organophilization is not enough to intercalate PE. Additionally, the peaks corresponding to PE appear unaffected, which means that the presence of the inorganic material does not alter the crystalline structure of PE. Note that variation of the mixing conditions inside the micromixer does not influence the immiscible structure. Mixing from solution was not attempted, since, we were not aware of common solvents at ambient temperature that could both dissolve polyethylene and disperse the organoclay and since comparison between blending in the extruder and solution mixing was not in the scope of the present study. These results verify that mixing of PE with organophilized layered inorganic material leads to phase separated systems as expected from the non-polar character of PE. It is clear that for the synthesis of PE/layered silicate nanocomposites one has to modify the interactions between the polymer and the inorganic surfaces.

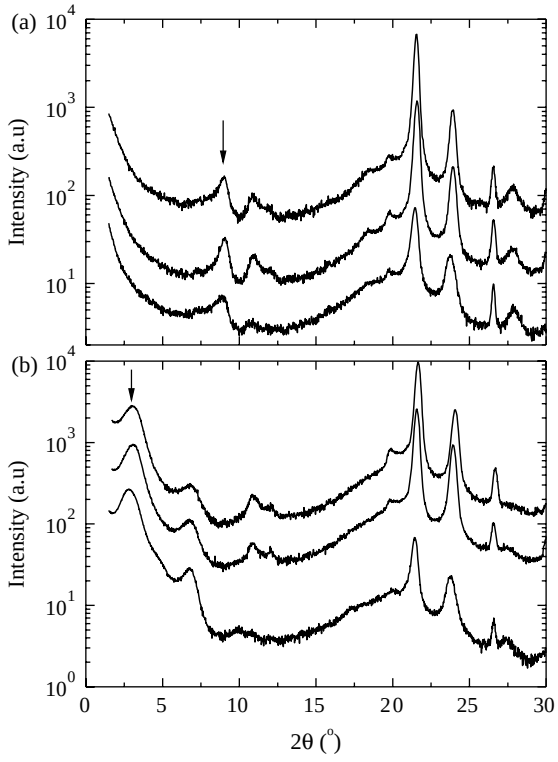

Fig. 2. (a) X-ray diffractograms of three-component PE hybrids containing NPE and 15 wt% Na^+MMT. From top to bottom the hybrids contain 1 wt% NPE-1, 1 wt% NPE-2 or 10% NPE-1. (b) X-ray diffractograms of three-component PE hybrids containing NPE and 15 wt% Dellite 72 T. From top to bottom the hybrids contain 1 wt% NPE-1, 1 wt% NPE-2 or 10% NPE-1. The curves are shifted for clarity.

A way to overcome this problem is to use compatilizing chains which will intercalate into the silicate galleries and will either play the role of polymeric surfactants or will be used to create an environment more friendly for the polymer. The first compatibilizer used, is a linear end-functionalized polyethylene with dimethyl ammonium chloride end groups, NPE. It was used as a polymeric surfactant in order to render the Na^+ montmorillonite organophilic. This molecule is essentially a polymeric cationic surfactant with a polyethylene tail that would enhance the miscibility with pure PE. The results of this attempt are shown in Fig. 2(a). Two different molecular weights (Table 1) of the additive were used and its concentration in the hybrid was varied between 1 and 10 wt%. The overall polymer/silicate composition was kept constant at 15 wt% clay in all cases. It is obvious that the presence of the additive does not affect the structure of the inorganic material since the characteristic diffraction peak is observed at exactly the same angle with the ones of the pure montmorillonite and the phase separated system of Fig. 1. This means that this additive, despite the presence of the cationic end-group, cannot intercalate into the clay's galleries, either due to its high molecular weight or due to the unfavorable interactions of the long PE tail of the 'surfactant' with the surfaces. It should be mentioned that the concentrations of the additive is enough for intercalation to be evident. One may object to the way this 'organophilization' was attempted. The usual organophilization using C_{12} or C_{18}-tail cationic surfactant is performed either in solution or in a solvent-free way where, in the latter, the tallow surfactants are in a state of paste. However, the present 'polymeric' surfactants are neither soluble in common solvents nor in a paste state. Thus, the

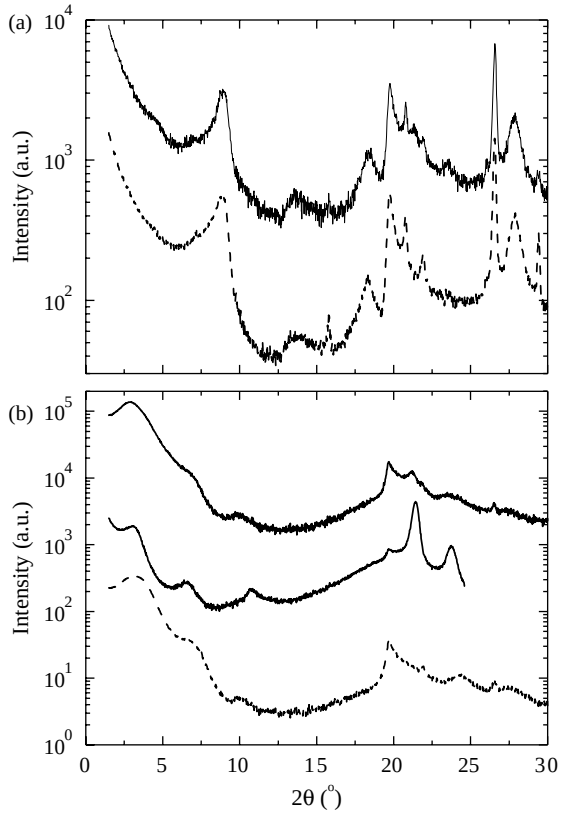

Fig. 3. (a) X-ray diffractograms of a hybrid containing PE-*g*-NPE (30 wt%) and Na^+MMT (70 wt%) with its respective clay (dashed line). (b) X-ray diffractograms of a binary hybrid containing PE-*g*-NPE (30 wt%) and Cloisite 20 A (70 wt%) at the top, a three-component hybrid containing (87 wt% (90 wt% PE + 10 wt% PE-*g*-NPE) + 13 wt% Cloisite 20 A) in the middle and the respective organoclay (dashed line). The curves are shifted for clarity.

procedure described above was necessary. Note, that similar polystyrene-based polymeric surfactants were able to organically modify the clay surfaces from a mixture of solvents [50]. Then, these polymeric surfactants were used as compatibilizers between an organophillized montmorillonite and polyethylene, i.e. as modifiers of the effective polarity of PE. Hybrids with 15 wt% Dellite 72 T and 1–10 wt% NPE, were synthesized. The X-ray diffractograms shown in Fig. 2(b) indicate once more that the additives were not successful in altering the structure of the organophilic silicates either.

One functional quaternary ammonium end group was, apparently, not enough to alter the clay structure or act as compatibilizer. Thus, another functional additive was synthesized, which possesses more functional ammonium groups distributed along the polymer chains. This was first utilized in the role of a polymeric surfactant. To that end it was used in relatively high concentration. This approach again led to immiscible systems: the interlayer distance of the hydrophilic silicate remained unaltered as shown in Fig. 3(a). More promising results were, however, obtained when this polymer was utilized with Cloisite 20 A in order to act as a modifier of the polyethylene polarity. Fig. 3(b) shows the X-ray data for two types of samples. One is a hybrid that comprised of 30 wt% of the multifunctional additive (used essentially as the polymer) and Cloisite 20 A. The results, as shown in Fig. 3(b), are similar with the ones of Fig. 3(a). There is only a very small decrease of the diffraction angle which could correspond to an increase of the interlayer distance of ~2.5 Å. The case is somehow different when all three components are used. The mixture consisted of 87 wt% (90 wt% PE + 10 wt% PE-*g*-NPE) + 13 wt% Cloisite 20 A and its diffractogram is shown also in Fig. 3(b). A significant drop of the intensity of the main peak is evident which, nevertheless, remains at the same position. At the same time there is an increase of the intensity at low angles, which indicates that there must be a degree of disorder and possible exfoliation in the hybrid. As will become more evident below, we believe that the difference in the behavior of these two hybrids is due to the different ratio of compatibilizer to organoclay, which will emerge as a very important parameter. In the first case this ratio was 0.43:1, whereas, in the second it was 0.67:1.

The effect of the second type of synthesized additive on altering the structure of the composites was more pronounced. It was anticipated that a diblock copolymer of polyethylene-*block*-poly(methacrylic acid), will intercalate into the galleries of the montmorillonite due to the polarity of the carboxyl groups of poly(methacrylic acid). This would bring the polyethylene block into the galleries making thus the environment much more friendly for polyethylene. Fig. 4 shows the X-ray diffractograms for hybrids where the organic/inorganic composition is kept constant but the amount of the copolymer additive is varied between 2–15 wt%. This way the ratio of copolymer to organoclay was varied from 0.13:1 to 1:1. It can be seen that for the lower copolymer concentration there

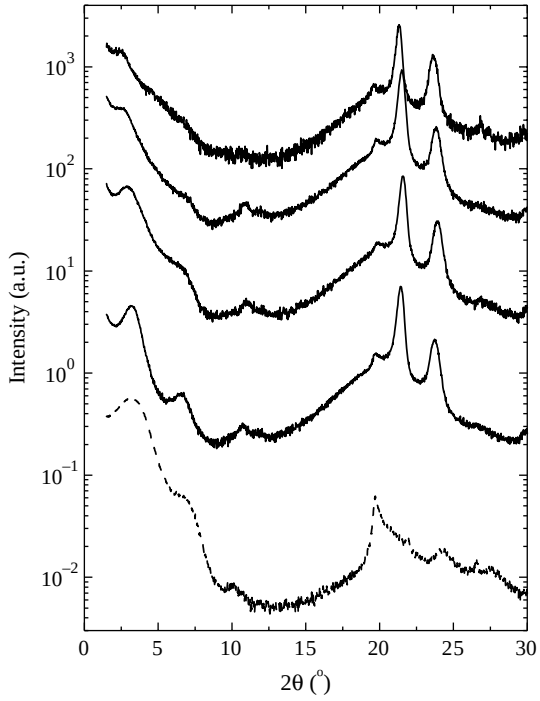

Fig. 4. X-ray diffractograms of three-component PE hybrids containing PE-*b*-PMAA and 13 wt% Cloisite 20 A. The PE-*b*-PMAA composition in the polymer is (from top to bottom) 15, 10, 6, and 2 wt%. The data for the respective organoclay are shown with the dashed line. The curves are shifted for clarity.

is not any change of the interlayer distance of Cloisite 20 A. The main peak is shown at $2\theta = 3.15°$ leading to $d_{001} = 28.0$ Å. It is noted, however, that the first and second order XRD peaks are better resolved than in the case of the pure organoclay indicating a better order in the composite sample that may be due to the polymer inside the silicate galleries reducing the randomness of the interstratification of the silicate layers. As the concentration of the additive increases, there is a gradual shift of the main diffraction peak to lower angles. At the higher concentration of the additive, i.e. 15 wt% (1:1), a very weak peak observed at $2\theta = 2.45°$ corresponds to $d_{001} = 36.0$ Å, which means an increase in the interlayer distance by ~8 Å. This increase is accompanied by a significant decrease of the intensity of the peak accompanied by an increase towards lower angles. Although, X-ray diffraction is a suitable technique to detect the intercalation of the polymer chains within the galleries of the inorganic material, it can only indirectly provide information about exfoliation of the layers [51]. In this case, however, we can conclude that most probably as the concentration of the PE-*b*-PMAA increases, there exist both intercalated and disorder or exfoliated regions [30,52]. In order to investigate whether it is simply the copolymer chains which intercalate or whether the polyethylene chains participate as well, a hybrid was synthesized that contained only PE-*b*-PMAA in 30/70 wt% relatively to organoclay. The mixing in this case was performed simply by heating in a vacuum oven and diffractograms were recorded for various annealing times. The system showed slow kinetics but the intercalation process was evident. At early annealing times there was the appearance of a double peak, one corresponding to the interlayer distance of the galleries of the empty organoclay and the other at $2\theta = 2.6°$ ($d_{001} = 34.0$ Å), similar to the one discussed above. With time the latter gained in amplitude and the former disappeared, as observed in other studies of intercalation kinetics [19]. It, thus, appears that it is the copolymer chains that intercalate and subsequently, these 'functional organoclays' exfoliate in the presence of the polyethylene matrix.

Finally, the third kind of additive used was the frequently utilized maleic anhydride-functionalized polyethylene (PE-*g*-MA) with MA content 0.85 wt%. This was used in concentrations ranging from 2.5 wt%, where PE-*g*-MA can be considered as an additive, up to 100 wt% where PE-*g*-MA is the polymer matrix. Both Dellite 72 T and Cloisite 20 A were used as inorganic materials. In all hybrids the concentration of the inorganic material was kept constant at 10 wt%. Since no differences were detected in the X-ray diffractograms between the two sets of nanocomposites, only the ones prepared with Dellite 72 T are discussed. Fig. 5 shows the X-ray diffractograms of all the composites where the curves have been shifted for clarity. For low concentrations of PE-*g*-MA (below 5 wt%), the data exhibit the characteristic peak of the parent organoclay signifying a phase separated system. As the relative concentration of PE-*g*-MA increases above 8 wt%, the diffraction peak appears to shift in the range $2\theta = 2.70$–$2.45°$, which means existence of intercalated structures with interlayer distance of $d_{001} = 32.7$–36.0 Å. At low angles, the intensity increases with decreasing scattering angle, which signifies the coexistence of exfoliated layers (together with intercalated ones). At 30 wt% PE-*g*-MA, there is only an indication of a shoulder in the data near $2\theta = 2.45°$. For even higher concentrations of PE-*g*-MA, there is no indication for the existence of a scattering peak of either the montmorillonite or of an intercalated system. The diffracted intensity shows a continuous decrease with increasing scattering angle which indicates that the structure has been destroyed due to the interactions of the polymer with the inorganic nanoparticles. This picture is valid for PE-*g*-MA concentrations from 49 to 100 wt%. Actually, it is the ratio of PE-*g*-MA to organoclay that determines the structure. For ratios of PE-*g*-MA to organoclay between 0 and 0.45:1, there is no change in the structure of the inorganic material, for ratios from 0.72:1 to 2.7:1 there is a mixture of intercalated and exfoliated structures whereas for ratios higher that 4.5:1 the structure of the organoclay has been completely destroyed and its layers are dispersed in the polymeric matrix [53]. This ratio determines the structure independently on whether the system is binary or ternary. For example, a composite which contains 60 wt% PE-*g*-MA and 40 wt% Dellite 72 T (compatibilizer to organoclay 1.5:1) shows an intercalated structure with a diffraction peak at 2.55°. A similar peak is observed for a three component system 90% (15% PE-*g*-MA + 85% PE) + 10% Dellite 72 T which contains a similar ratio of compatibilizer to silicate (1.35:1). At the same time, hybrids containing an even larger ratio of 90%

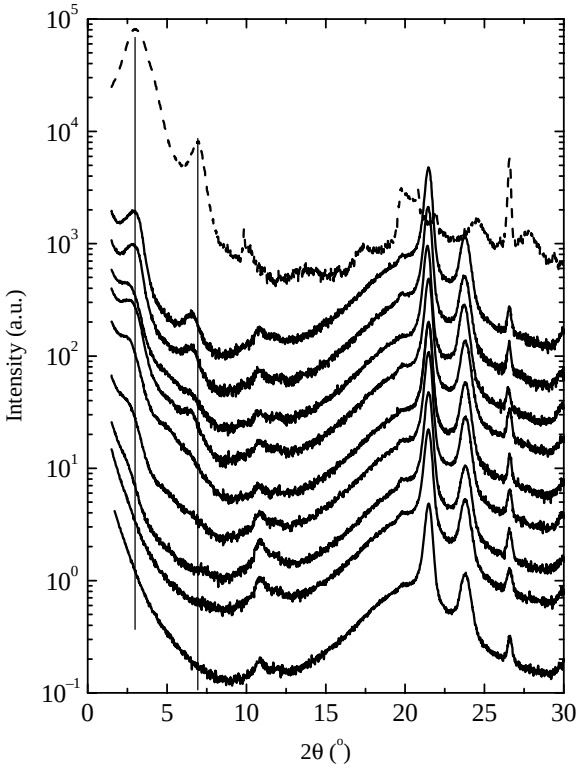

Fig. 5. X-ray diffractograms of three-component PE hybrids containing PE-*g*-MA and 10 wt% organoclay Dellite 72 T with different relative compositions of PE to PE-*g*-MA. The solid lines from top to bottom correspond to PE/PE-*g*-MA = 97.5/2.5, 95/5, 92/8, 85/15, 82/18, 80/20, 70/30, 51/49, 0/100. The data for the respective organoclay are shown for comparison with the dashed line. The curves are shifted for clarity.

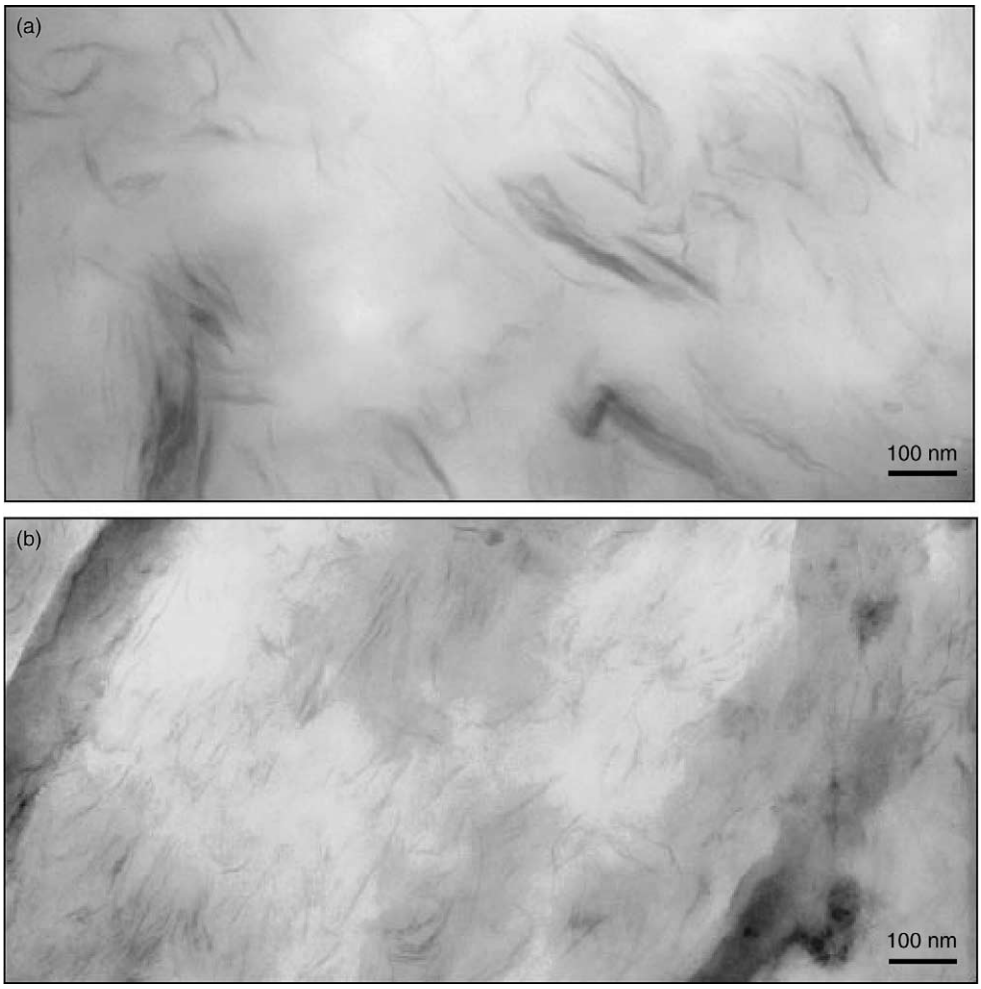

Fig. 6. Transmission electron microscopy images of two PE hybrids containing PE-*g*-MA and 10 wt% organoclay Dellite 72 T. (a) PE/PE-*g*-MA = 85/15. (b) PE/PE-*g*-MA = 51/49. The dark lines represent the edges of the silicate layers and the white region the polymeric matrix.

PE-*g*-MA to 10% Dellite 72 T (9:1) show exfoliated structure, as expected.

The importance of the compatibilizer to the organoclay ratio in determining the structure is confirmed further by transmission electron microscopy. Fig. 6 shows TEM images of two hybrids containing 10% Dellite 72 T and ratios of PE-*g*-MA compatibilizer to organoclay 1.35:1 (a) and 4.5:1 (b). The dark lines represent the edges of the silicate layers and the white region the polymeric matrix. Clear differences are observed between the two systems. It is evident that a coexistence is observed in (a) of clay particles retaining the layered intercalated structure and clay platelets dispersed within the polymer matrix. For the higher concentration of compatibilizer in (b), a uniform dispersion of exfoliated platelets is observed. These results are in excellent agreement with the X-ray diffraction data.

The investigation of the structure of the micro- or nanocomposites that can be obtained by the modification of the polyolefin/silicate interactions was conducted in order to understand and improve the properties of the resulting hybrids. The rheological properties of the micro- or nanocomposites are of particular importance, since they determine the processability of the composites [35–38,40]. Moreover, it is of interest whether there is a one-to-one correspondence of properties to structure with respect to being able to understand the structure utilizing rheology. It has been reported that rheology may provide information on the structure of the micro- or nanocomposites [54]. Wagener and Reisinger investigated the frequency dependence of the complex viscosity for a number of nanohybrids and proposed that this dependence correlates well with the micro- or nanostructure. Thus, the rheological properties were investigated for the polyethylene composites, where X-ray diffraction has provided evidence of the existence of all the three types of structures.

First, oscillatory rheological measurements at low frequencies were employed as a function of temperature in order to investigate the crystallization of PE and its composites. Fig. 7(a) shows the temperature dependence of the storage and loss moduli at $\omega = 10$ rad/s, for polyolefin homopolymer as the temperature decreases towards crystallization by 0.5 °C/min. G' and G'' increase very weakly with decreasing temperature for high temperatures. The significant upturn at lower temperatures signifies the first order crystallization transition. The temperature, 103 °C, at the inflection point of the modulus versus temperature, is identified as the crystallization temperature of polyethylene in agreement with the

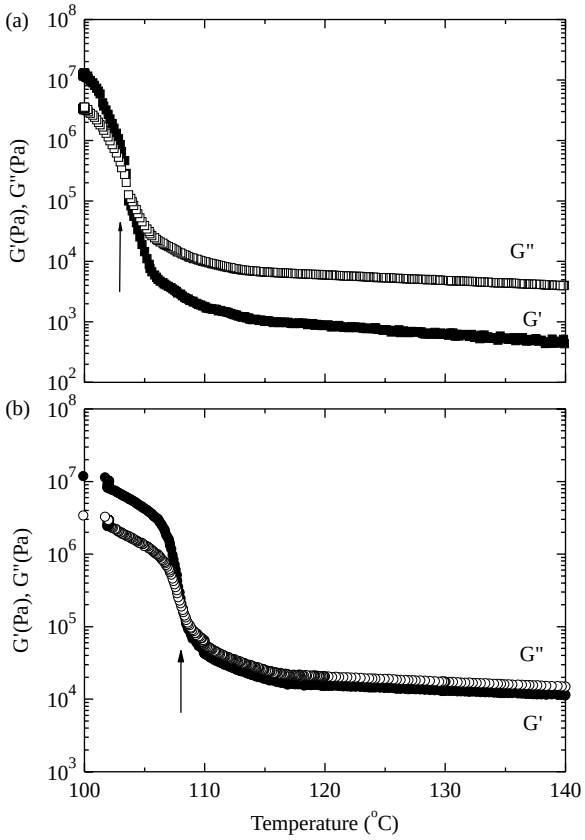

Fig. 7. Temperature dependence of the storage modulus, G' (solid symbols), and the loss modulus, G'' (open symbols) of (a) PE and (b) a three-component PE hybrid containing PE-*g*-MA and 10 wt% Dellite 72 T with a ratio PE/PE-*g*-MA85/15 for which a mixture of intercalated and exfoliated structure exists. The arrows indicate the crystallization temperatures (Table 3).

DSC results (Table 3). Fig. 7(b) depicts the respective data for a hybrid which shows a mixture of intercalated and exfoliated structure. The crystallization temperature is now estimated at 108 °C again in agreement with DSC. This increase is attributed to the presence of the inorganic material which may affect the nucleation rate even at reduced undercooling in agreement with recent reports [36]. It is noted that an immiscible hybrid exhibits a rheologically estimated crystallization temperature of 108 °C as well (Table 3).

Fig. 8(a) shows the frequency dependence of G' and G'' together with the viscosity η at 140 °C obtained by dynamic frequency sweeps for the PE homopolymer and for a micro-

Table 3
Melting and crystallization temperatures

Sample	T_m (DSC) (°C)	T_c (DSC) (°C)	T_c (Rheology) (°C)
PE	129	102	103
PE-*g*-MA	124	99	
87 wt% PE+13 wt% Dellite 72 T	128	110	108
90% (15 wt% PE-*g*-MA+85 wt% PE)+10 wt% Dellite 72 T	128	111	108
90% (49 wt% PE-*g*-MA+51% PE)+10 wt% Dellite 72 T	127	106	

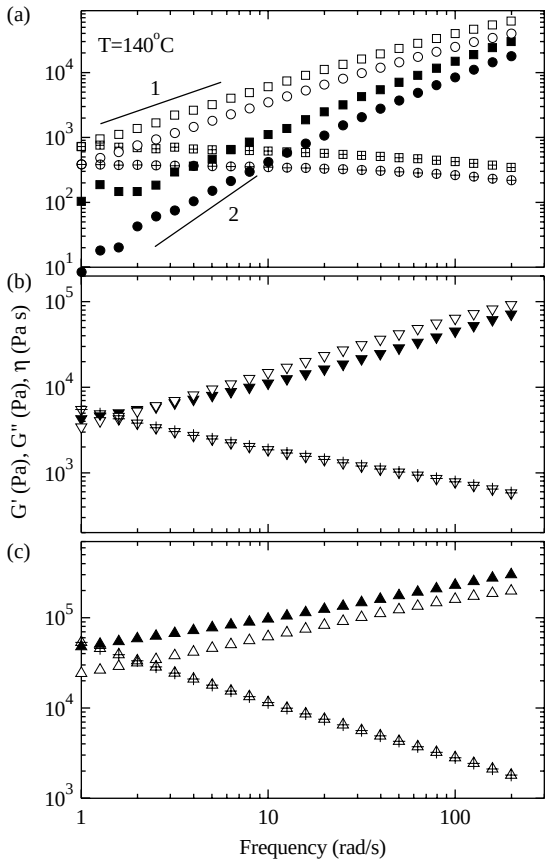

Fig. 8. (a) Dynamic frequency sweep measurements at 140 °C of pure PE (circles) and a hybrid containing 87 wt% PE+13 wt% Dellite 72 T (squares), (b) Dynamic frequency sweep measurements at 140 °C of a three-component PE hybrid containing PE-*g*-MA and 10 wt% Dellite 72 T with PE/PE-*g*-MA= 85/15 (inverted triangles). (c) Dynamic frequency sweep measurements at 140 °C of a three-component PE hybrid containing PE-*g*-MA and 10 wt% Dellite 72 T with PE/PE-*g*-MA=51/49 (up triangles). Storage modulus G' (solid symbols), loss modulus G'' (open symbols), viscosity η (crossed symbols).

composite with Dellite 72 T (immiscible system). These measurements are obtained at temperatures far above the crystallization so that crystallization effects do not interfere with the results reported here. The data for the PE homopolymer and for the immiscible micro-composite are very similar. The G' and G'' moduli exhibit the expected ω^{-2} and ω^{-1} dependence on frequency in the flow regime, whereas the viscosity exhibits a low freuency plateau. It is simply the values of the moduli and the viscosity that are higher by a factor of 2 in the micro-composite. Moreover, time–temperature superposition holds for all temperatures up to very close to the crystallization temperature. Fig. 8(c) shows the frequency dependence of G', G'' and η at 140 °C for the exfoliated system containing 10% Dellite 72 T and polymer with 49 wt% PE-*g*-MA and 51 wt% PE. The picture is significantly different than that of Fig. 8(a). The storage modulus, G', attains values that are higher than the loss modulus, G'', (for all temperatures) whereas both G' and G'' display weak frequency dependencies indicative of a solid-like behavior. The dynamic moduli data for a hybrid, which contains both intercalated and exfoliated platelets (Fig. 8(b)), show an intermediate behavior: G'' is

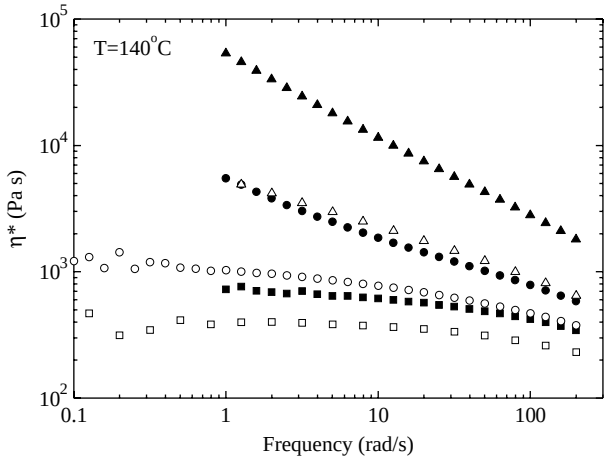

Fig. 9. Frequency dependence of the complex viscosity of various systems at 140 °C. (□) polyethylene PE, (○) a binary mixture containing 85 wt% PE and 15 wt% PE-*g*-MA, (△) a binary mixture containing 51 wt% PE and 49% PE-*g*-MA, (■) a binary hybrid containing 85 wt% PE + 15 wt% Dellite 72 T, (●) a three-component hybrid containing PE-*g*-MA and 10 wt% Dellite 72 T with PE/PE-*g*-MA = 85/15, and (▲) a three-component hybrid containing PE-*g*-MA and 10 wt% Dellite 72 T with PE/PE-*g*-MA = 51/49.

slightly higher than G' with both exhibiting very weak frequency dependencies. This picture is very similar to results on polystyrene (PS) nanocomposites. It is well known that PS intercalates in organophilic montmorillonite whereas it results in a phase separated system when it is mixed with hydrophilic clays. The rheological response of PS homopolymer and the PS/hydrophilic clay is very similar showing a liquid-like behavior. This situation is quantitatively and qualitatively altered for an intercalated system of PS with organophilic montmorillonite (e.g. Cloisite 20 A). Values of the storage modulus are higher than those of the loss modulus for all temperatures measured, indicating, for this system as well, a solid-like behavior in the nanocomposite.

The use of PE-*g*-MA as compatibilizer allows the synthesis of systems with all three types of structures. Fig. 9 shows the frequency dependence of the complex viscosity measured at 140 °C for three different pair of systems. In each pair one specimen contains 15 wt% of the organoclay Dellite 72 T (filled symbols) while the other belongs to the neat polymer. The three different pairs correspond to an immiscible system (PE/organoclay Fig. 7), an exfoliated system (containing 4.5:1 compatibilizer to organoclay) and a system where only partial exfoliation and slight intercalation can be inferred from the X-ray diffraction data (containing 1.4:1 compatibilizer to organoclay in Fig. 5). For comparison the data for the respective polymer (or mixtures), i.e. in the absence of the organoclay is also included. The different composite structures are clearly reflected on the rheological behavior. The liquid-like response (frequency independent complex viscosity) is only observed for the PE homopolymer, the immiscible PE/organoclay hybrid and the 85:15 mixture of PE to PE-*g*-MA. The behavior for the exfoliated system is entirely different corresponding to a solid-like response of both G' and G'' (Fig. 8(c)), whereas, the behavior of the third system is intermediate between the two extremes. The change in the behavior may be quantified by evaluating the shear-thinning exponent n by analyzing the data in terms of a $\eta^* = A\omega^n$ dependence [54]. For a liquid-like behavior $n \sim 0$, whereas for a solid-like response $n \sim -1$. Wagener and Reisinger proposed to use the value of n as a measure of the degree of exfoliation. In that, it was explicitly assumed that exfoliation leads to a percolated structure which results to a solid-like behavior. Indeed, an increase of the shear thinning exponent is observed with the increase of the degree of exfoliation, when the rheological data are correlated to the X-ray diffraction results. n is zero for the homopolymer PE and $n = -0.1$ for the immiscible 87% PE/13% Dellite 72 T hybrid, whereas $n = -0.4$ for the slightly exfoliated 91% (15% PE-*g*-MA + 85% PE) + 9% Dellite 72 T and $n = -0.65$ for the completely exfoliated 91% (51% PE-*g*-MA + 49% PE) + 9% Dellite 72 T. Care should be used in analyzing the data since the shear thinning exponent does vary with the polymer matrix. The shear thinning exponent is very low ($n = -0.1$) for 85 wt% PE/15 wt% PE-*g*-MA and it becomes $n = -0.39$ for 49 wt% PE/51 wt% PE-*g*-MA. However, in both cases the frequency dependence is much weaker for the blend of polymers than that for the three-component hybrids. Therefore, the 'shear thinning exponent' can indeed be correlated with the structure of the system since it essentially describes the transition from a liquid-like behavior of the immiscible micro-composites to the solid- or gel-like behavior of the exfoliated nanocomposites due to the percolated structure of the nanohybrids.

4. Concluding remarks

The morphology of polyethylene/layered silicate micro- and nanocomposites can be controlled systematically by modifying the interactions between the organic and the inorganic nanoparticles. This is accomplished via the utilization of three different types of additives specifically designed to play the role of a polymeric surfactant or a compatibilizer. Immiscible, intercalated and exfoliated structures can be obtained in a controlled way where the final morphology is determined by the kind of the additive and its concentration in the mixture. The important factor controlling the structure is the ratio of additive to inorganic. For PE-*g*-MA as an additive, ratios less than 0.45:1 result in immiscible systems, whereas ratios higher than 4.5:1 lead to complete exfoliation; mixtures of intercalated and exfoliated structures are obtained for the intermediate ratios. The rheological behavior of the hybrids changes from a liquid-like to a solid-like when the system's structure varies from a phase separated state to an intercalated and an exfoliated one possibly due to percolation. The frequency dependence of the complex viscosity can, thus, be utilized as a measure of the degree of exfoliation in the hybrids.

Acknowledgements

The authors would like to acknowledge that part of this research was sponsored by the Greek General Secretariat of Research and Technology in the framework of PAVET Programme (Project No 00BE137).

References

[1] Mitchell CA, Bahr JL, Arepalli S, Tour JM, Krishnamoorti R. Macromolecules 2002;35(23):8825–30.
[2] Granick S, Kumar SK, Amis EJ, Antonietti M, Balazs AC, Chakraborty AK, et al. J Polym Sci, Part B: Polym Phys 2003;41(22): 2755–93.
[3] Pinnavaia TJ, Beau GW. Polymer–clay nanocomposites. West Sussex: Wiley; 2000.
[4] Giannelis EP, Krishnamoorti R, Manias E. Adv Polym Sci 1999;138: 107–47.
[5] Alexandre M, Dupois P. Mater Sci Eng R 2000;28(1-2):1–63.
[6] Sinha Ray S, Okamoto M. Prog Polym Sci 2003;28(11):1539–641.
[7] Vaia RA, Price G, Ruth PN, Nguyen HT, Lichtenhan. J Appl Clay Sci 1999;15(1–2):67–92.
[8] Biswas M, Sinha Ray S. Adv Polym Sci 2001;155:167–221.
[9] Schmidt D, Shah D, Giannelis EP. Curr Opin Solid State Mater Sci 2002; 6(3):205–12.
[10] Giannelis EP. Appl Organomet Chem 1998;12(10-11):675–80.
[11] Bharadwaj RK. Macromolecules 2001;34(26):9189–92.
[12] Messersmith PB, Giannelis EP. J Polym Sci, Part A: Polym Chem 1995; 33(7):1047–57.
[13] Yano K, Usuki A, Okada A, Kurauchi T, Kamigaito O. J Polym Sci, Part A: Polym Chem 1993;31:2493–8.
[14] Gilman JW. Appl Clay Sci 1999;15(1-2):31–49.
[15] Gilman JW, Jackson CL, Morgan AB, Harris Jr R, Manias E, Giannelis EP, et al. Chem Mater 2000;12(7):1866–73.
[16] Sinha Ray S, Yamada K, Okamoto M, Ueda K. Nano Lett 2002;2(10): 1093–6.
[17] Vaia RA, Jandt KD, Kramer EJ, Giannelis EP. Chem Mater 1996;8(11): 2628–35.
[18] Vaia RA, Sauer BB, Tse OK, Giannelis EP. J Polym Sci, Part B: Polym Phys 1997;35(1):59–67. Hackett E, Manias E, Giannelis EP. Chem Mater 2000;12(8):2161–7. Shen Z, Simon GP, Cheng Y. Eur Polym J 2003; 39(9):1917–24.
[19] Vaia RA, Jandt KD, Kramer EJ, Giannelis EP. Macromolecules 1995; 28(24):8080–5.
[20] Usuki A, Kojima Y, Kawasumi M, Okada A, Fukushima Y, Kurauchi T, et al. J Mater Res 1993;8(5):1179–84.
[21] Vaia RA, Giannelis EP. Macromolecules 1997;30(25):7990–9.
[22] Balazs AC, Singh C, Zhulina E. Macromolecules 1998;31(23):8370–81.
[23] Zhulina E, Singh C, Balazs AC. Langmuir 1999;15(11):3935–43.
[24] Bains AS, Boek ES, Coveney PV, Williams SJ, Akbar MV. Mol Simul 2001;26(2):101.
[25] Vaia RA, Giannelis EP. Macromolecules 1997;30(25):8000–9.
[26] Vohra VR, Schmidt DF, Ober CK, Giannelis EP. J Polym Sci, Polym Phys 2003;41(24):3151–9.
[27] Kato M, Usuki A, Okada A. J Appl Polym Sci 1997;66(9):1781–5.
[28] Kawasumi M, Hasegawa N, Kato M, Usuki A, Okada A. Macromolecules 1997;30(20):6333–8.
[29] Hasegawa N, Kawasumi M, Kato M, Usuki A, Okada A. J Appl Polym Sci 1998;67(1):87–92.
[30] Manias E, Touny A, Wu L, Stawhecker K, Lu B, Chung TC. Chem Mater 2001;13(10):3516–23.
[31] Nam PH, Maiti P, Okamoto M, Kotaka T, Hasegawa N, Usuki A. Polymer 2001;42(23):9633–40.
[32] Solomon MJ, Almusallam AS, Seefeldt KF, Somwangthanaroj A, Varadan P. Macromolecules 2001;34(6):1864–72.
[33] Galgali G, Ramesh C, Lele A. Macromolecules 2001;34(4):852–8.
[34] Okamoto M, Nam PH, Maiti P, Kotaka T, Hasegawa N, Usuki A. Nano Lett 2001;1(6):295–8.
[35] Hotta S, Paul DR. Polymer 2004;45(22):7639–54.
[36] Gopakumar TG, Lee JA, Kontopoulou M, Parent JS. Polymer 2002; 43(20):5483–91.
[37] Lee J, Kontopoulou M, Parent JS. Polymer 2004;45(19):6595–600.
[38] Wang KH, Choi MH, Koo CM, Xu M, Chung IJ, Jang MC, et al. J Polym Sci, Part B: Polym Phys 2002;40(14):1454–63.
[39] Wang KH, Choi MH, Koo CM, Choi YS, Chung IJ. Polymer 2001;42(24): 9819–26.
[40] Koo CM, Ham HT, Kim SO, Wang KH, Chung IJ, Kim DC, et al. Macromolecules 2002;35(13):5116–22. Koo CM, Kim SO, Chung IJ. Macromolecules 2003;36(8):2748–57.
[41] Liu X, Wu Q. Polymer 2001;42(25):10013–9.
[42] Alexandre M, Dupois P, Sun T, Garces JM, Jerome R. Polymer 2002; 43(8):2123–32.
[43] Shin S-YA, Simon LC, Soares JBP, Scholz G. Polymer 2003;44(18): 5317–21.
[44] Hadjichristidis N, Iatrou H, Pispas S, Pitsikalis M. J Polym Sci, Part A: Polym Chem 2000;38(18):3211–34.
[45] Pispas S, Pitsikalis M, Hadjichristidis N, Dardani P, Morandi F. Polymer 1995;36(15):3005–11.
[46] Pispas S, Siakali-Kioulafa E, Hadjichristidis N, Mavromoustakos T. Macromol Chem Phys 2002;203(10–11):1317–27.
[47] Mark JE, editor. Physical properties of polymers handbook. Woodbury, NY: AIP Press; 1996.
[48] The diffractogram of montmorillonite measured as received shows the main peak at $2\theta = 7.2^\circ$ corresponding to $d_{001} = 12.3$ Å, which indicates that simply the presence of water increases the montmorillonite interlayer distance by ~ 2.5 Å. Moreover, after the heating of the material and the removal of the water, the diffraction peak is significantly sharper, indicating better coherence of the layers.
[49] Reynolds RC. In: Post DLBJE, editor. Reviews in mineralogy, vol. 20. Washington, DC: The Mineralogical Society of America; 1989. p. 145–83.
[50] Beter FL, Beck Tan NC, Dasgupta A, Galvin ME. Chem Mater 2002; 14(7):2983–8.
[51] Vaia RA, Liu W. J Polym Sci, Polym Phys 2002;40(15):1590–600.
[52] Kotek J, Kelnar I, Studenovsky M, Baldrian J. Polymer 2005;46(13): 4876–81.
[53] A similar behavior is observed when Cloisite 20 A is utilized instead Dellite 72 T, where an increase in the interlayer distance of about 5 Å is observed for additive concentrations between 5 and 30 wt%, whereas, for higher concentrations exfoliated structures are obtained.
[54] Wagener R, Reisinger TJG. Polymer 2003;44(24):7513–8.